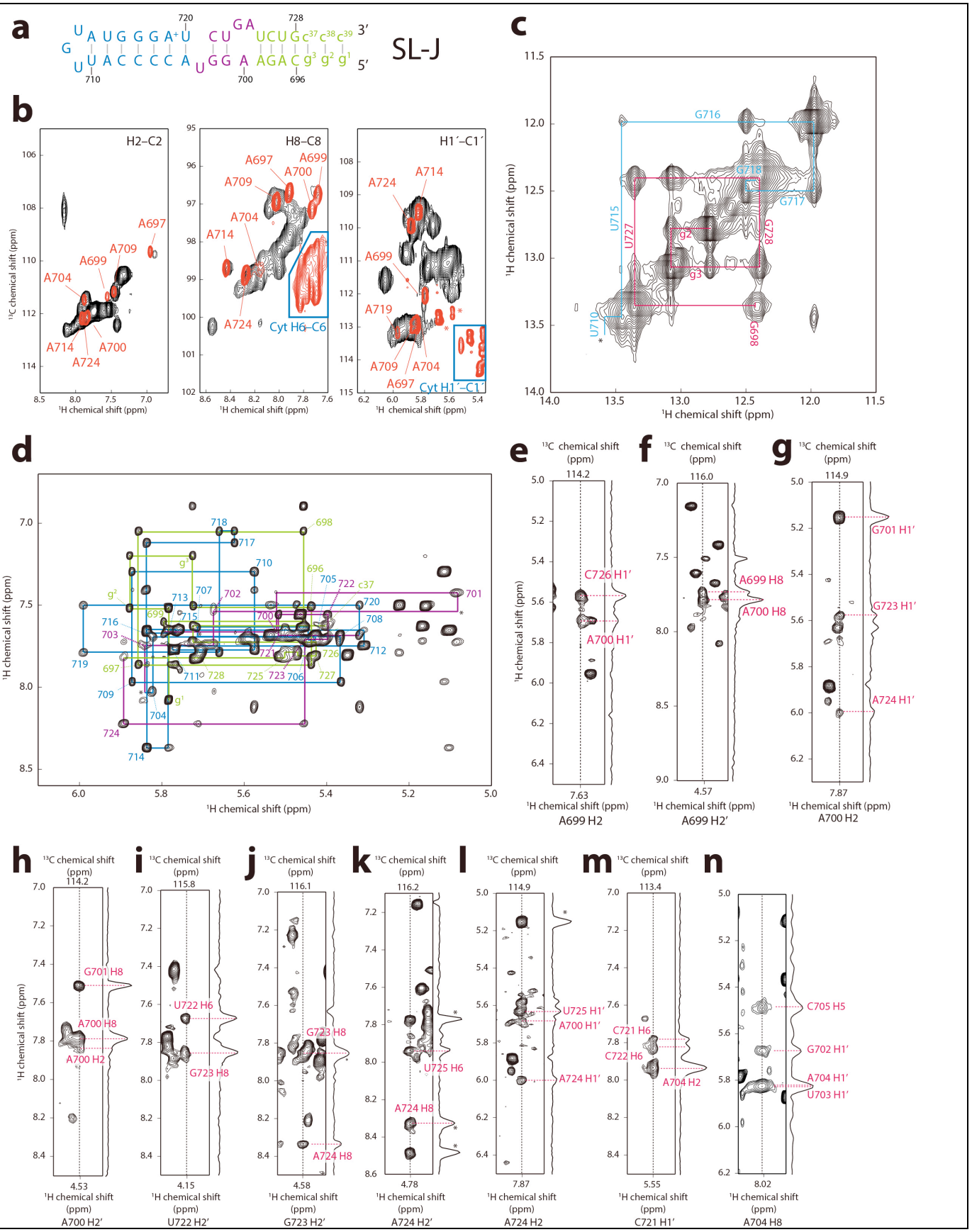
a
SL-J
b
H2–C2
H8–C8
H1′–C1′
Cyt H6–C6
Cyt H1′–C1′
c
d
e
f
g
h
i
j
k
l
m
n

Supplementary Figure 1

NMR signal assignments and structural analysis of SL-J

(**a**) Sequence and NMR-derived secondary structure of SL-J. Colors indicate the sequential assignment in (**d**). (**b**) Overlay of the Ade H2–C2, H8–C8, and H1′–C1′ regions of ^{1}H-^{13}C HMQC spectra of [^{13}C,^{15}N-Ade/Cyt] SL-J (red) and [^{13}C,^{15}N-Ade] J-K (black). Asterisks indicate signals due to heterogenous termini in the RNA transcript. (**c**) ^{1}H-^{1}H NOESY spectrum of the imino proton region with the imino proton walk of SL-J that supports the secondary structure of SL-J. The lower and upper stem walks are shown with red and cyan lines, respectively. (**d**) Sequential walk of H1′–H6 (pyrimidine) or H1′–H8 (purine) connectivity for the assignments. Labels show the intraresidual H1′–H6 or H1′–H8 signals of each residue. Green and cyan, and purple lines represent the sequential walk of the segments shown in the same colors in (**a**). Asterisks indicate that the signals are below the threshold. (**e-m**) NOESY strips derived from ^{13}C-edited HMQC-NOESY 3D spectra of [^{13}C,^{15}N-Ade/Cyt] or [^{13}C,^{15}N-Gua/Uri] labeled SL-J for the structural characterization of the bulges. Asterisks indicate that the signals are not in the same plane in the ^{13}C dimension and not connected to the spin system, or that the intensities of the signals are not determined because of overlaps. (**n**) A NOESY strip derived from ^{1}H-^{1}H NOESY spectrum of SL-J for the structural characterization of the U703 bulge.

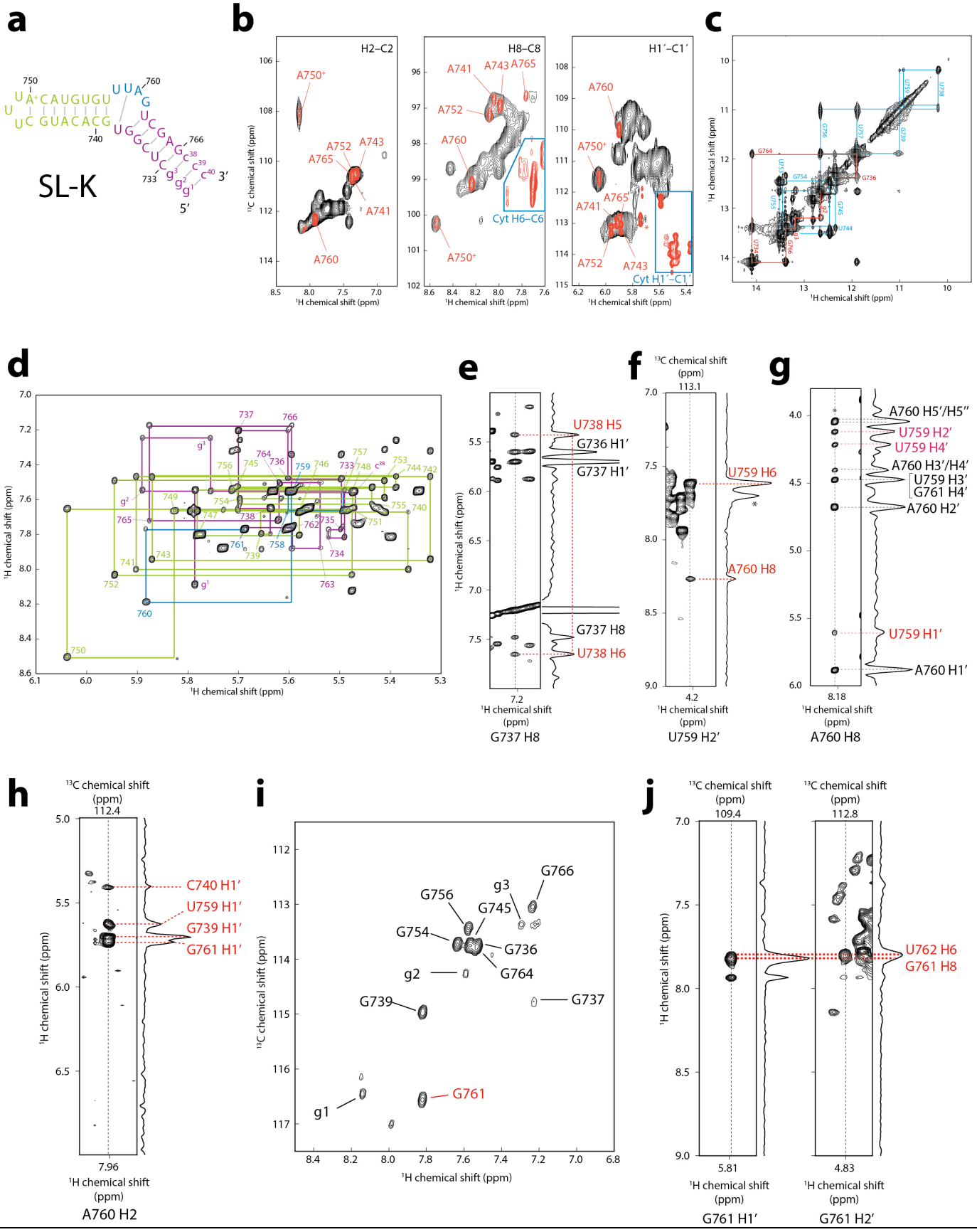
a
SL-K
5′
3′
b
H2–C2
H8–C8
H1′–C1′
Cyt H6–C6
Cyt H1′–C1′
¹³C chemical shift (ppm)
¹H chemical shift (ppm)
c
¹H chemical shift (ppm)
d
¹H chemical shift (ppm)
e
U738 H5
G736 H1′
G737 H1′
G737 H8
U738 H6
¹H chemical shift (ppm)
G737 H8
f
¹³C chemical shift (ppm)
113.1
U759 H6
A760 H8
¹H chemical shift (ppm)
U759 H2′
g
A760 H5′/H5″
U759 H2′
U759 H4′
A760 H3′/H4′
U759 H3′
G761 H4′
A760 H2′
U759 H1′
A760 H1′
¹H chemical shift (ppm)
A760 H8
h
¹³C chemical shift (ppm)
112.4
C740 H1′
U759 H1′
G739 H1′
G761 H1′
¹H chemical shift (ppm)
7.96
¹H chemical shift (ppm)
A760 H2
i
¹³C chemical shift (ppm)
¹H chemical shift (ppm)
G766
g3
G756
G745
G754
G736
g2
G764
G739
G737
G761
g1
j
¹³C chemical shift (ppm)
109.4
¹³C chemical shift (ppm)
112.8
U762 H6
G761 H8
¹H chemical shift (ppm)
5.81
¹H chemical shift (ppm)
G761 H1′
4.83
¹H chemical shift (ppm)
G761 H2′

Supplementary Figure 2

NMR signal assignments and structural analysis of SL-K

(**a**) Sequence and NMR-derived secondary structure of SL-K. Colors indicate the sequential assignment in (**d**). (**b**) Overlay of the Ade H2–C2, H8–C8, and H1′–C1′ regions of ^{1}H-^{13}C HMQC spectra of [^{13}C,^{15}N-Ade/Cyt] SL-K (red) and [^{13}C,^{15}N-Ade] J-K (black). Asterisks indicate signals due to heterogenous termini in the RNA transcript. (**c**) ^{1}H-^{1}H NOESY spectrum of the imino proton region and imino proton walk of SL-K that supports the secondary structure of SL-K. The lower and upper stem walks are shown with red and cyan lines, respectively. The NOE signals between upfield shifted imino protons from U738 and U759 indicate a non-canonical basepair formed by these residues. (**d**) Sequential walk of H1′–H6 (pyrimidine) or H1′–H8 (purine) connectivity for the assignments. Labels show the intraresidual H1′–H6 or H1′–H8 signals of each residue. Green, cyan, and purple lines represent the sequential walk of the segments shown in the same colors in (**a**). Asterisks indicate that the signals are below the threshold. (**e, g**) NOESY strips derived from ^{1}H-^{1}H NOESY spectrum of SL-K for the structural characterization of the bulges. (**f, h, j**) NOESY strips derived from ^{13}C-edited HMQC-NOESY 3D spectra of [^{13}C,^{15}N-Ade/Cyt] or [^{13}C,^{15}N-Gua/Uri] labeled SL-K for the structural characterization of the bulges. The asterisk in (**f**) indicates that the signal is not in the same plane in the ^{13}C dimension and not connected to the spin system. (**i**) The Gua H8–C8 region of ^{1}H-^{13}C HMQC spectrum of [^{13}C,^{15}N-Gua/Uri] SL-K.

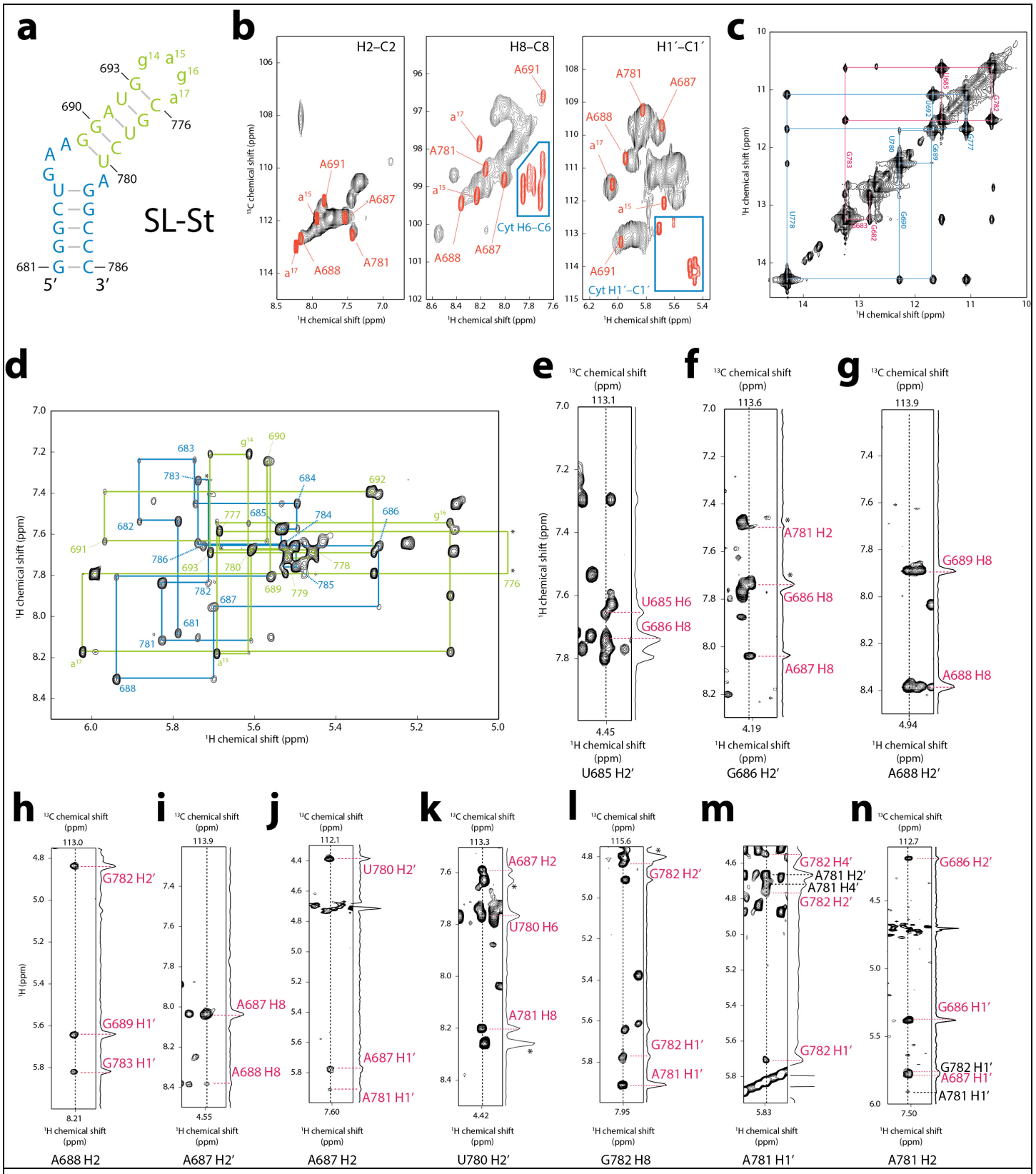

Supplementary Figure 3

NMR signal assignments and structural analysis of SL-St

(**a**) Sequence and NMR-derived secondary structure of SL-St. Colors indicate the sequential assignment in (**d**). (**b**) Overlay of the Ade H2–C2, H8–C8, and H1′–C1′ regions of ^{1}H-^{13}C HMQC spectra of [^{13}C,^{15}N-Ade/Cyt] SL-St (red) and [^{13}C,^{15}N-Ade] J-K (black). **(c)** ^{1}H-^{1}H NOESY spectrum of the imino proton region and imino proton walk of SL-St that supports the secondary structure of SL-St. The lower and upper stem walks are represented in red and cyan, respectively. (**d**) Sequential walk of H1′–H6 (pyrimidine) and H1′–H8 (purine) connectivity for the assignments. Labels show the intraresidual H1′–H6 (pyrimidine) or H1′–H8 (purine) signals of each residue. Green and cyan lines represent the sequential walk of the segments shown in the same colors in (**a**). Asterisks indicate that the signals are below the threshold. (**e-l, n**) NOESY strips derived from ^{13}C-edited HMQC-NOESY 3D spectra of [^{13}C,^{15}N-Ade/Cyt] and [^{13}C,^{15}N-Gua/Uri] labeled SL-St for the structural characterization of the bulges. Asterisks indicate that the signals are not in the same plane in the ^{13}C dimension and not connected to the spin system, or that the intensities of the signals are not determined because of overlaps. (**m**) NOESY strip derived from ^{1}H-^{1}H NOESY spectrum of SL-St for the structural characterization of the bulges.

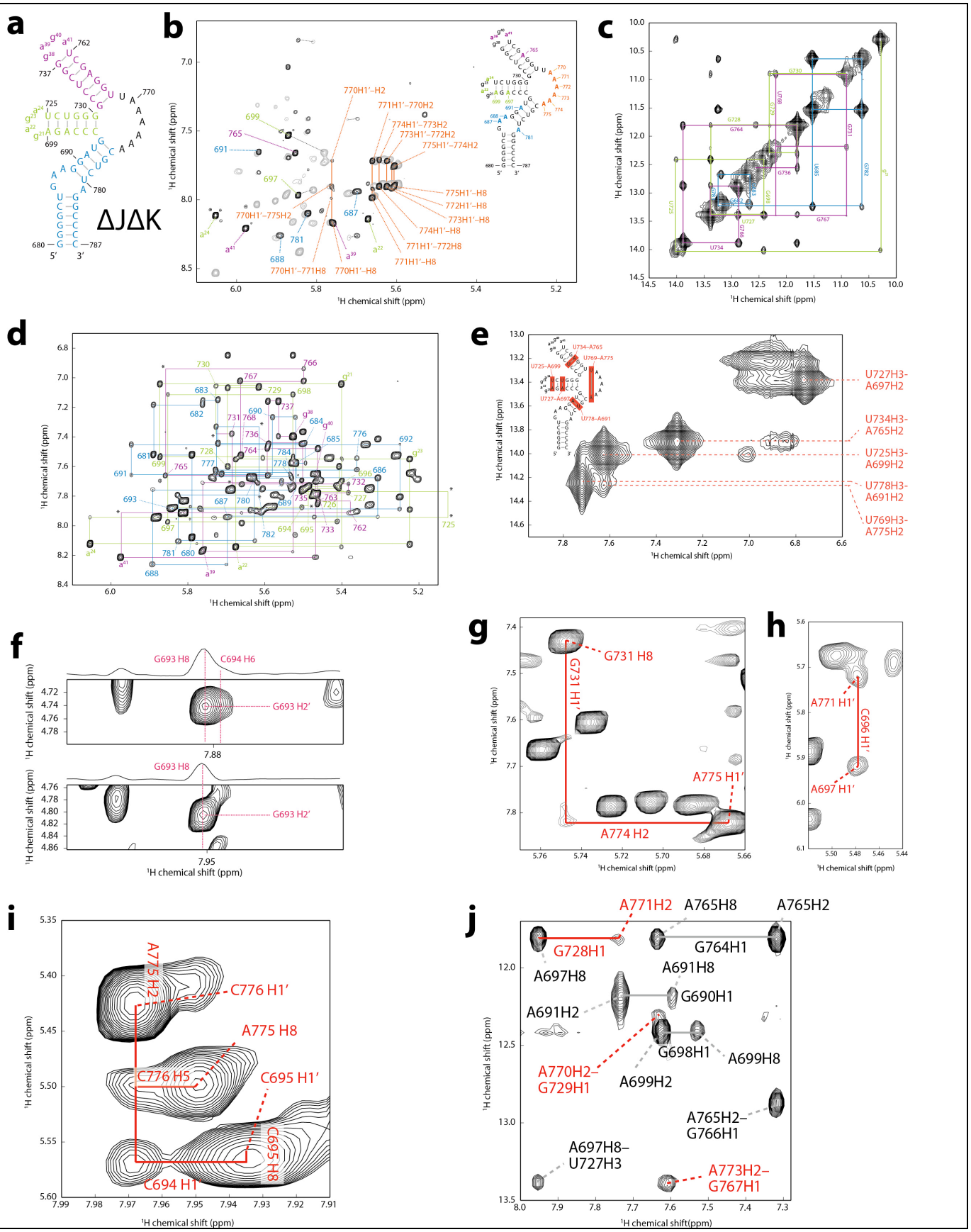
a
ΔJΔK
b
770H1′–H2
771H1′–770H2
774H1′–773H2
773H1′–772H2
775H1′–774H2
775H1′–H8
772H1′–H8
773H1′–H8
774H1′–H8
771H1′–772H8
771H1′–H8
770H1′–775H2
770H1′–771H8
770H1′–H8
¹H chemical shift (ppm)
c
¹H chemical shift (ppm)
d
¹H chemical shift (ppm)
e
U727H3-A697H2
U734H3-A765H2
U725H3-A699H2
U778H3-A691H2
U769H3-A775H2
¹H chemical shift (ppm)
f
G693 H8
C694 H6
G693 H2′
7.88
7.95
¹H chemical shift (ppm)
g
G731 H8
G731 H1′
A775 H1′
A774 H2
¹H chemical shift (ppm)
h
A771 H1′
G696 H1′
A697 H1′
¹H chemical shift (ppm)
i
A775 H2
C776 H1′
A775 H8
C776 H5
C695 H1′
C695 H8
C694 H1′
¹H chemical shift (ppm)
j
A771H2
A765H8
A765H2
G728H1
G764H1
A697H8
A691H8
G690H1
A691H2
G698H1
A699H8
A770H2–
G729H1
A699H2
A765H2–
G766H1
A697H8–
U727H3
A773H2–
G767H1
¹H chemical shift(ppm)

Supplementary Figure 4

NMR signal assignments and structural analysis of ΔJΔK

(**a**) Sequence and NMR-derived secondary structure of ΔJΔK. Colors indicate the sequential assignment in (**c**). (**b**) Overlay of the ^{1}H-^{1}H NOESY spectra of [u-^{2}H,{H1′,H2′,H2,H8}-Ade] ΔJΔK (black) and [u-^{2}H,{H1′,H2′,H2,H8}-Ade] J-K (gray). (**c**) ^{1}H-^{1}H NOESY spectrum of the imino proton region and imino proton walk of ΔJΔK that supports the secondary structure of ΔJΔK. The imino walks are shown with red, cyan, and purple lines, respectively. (**d**) Sequential walk of H1′–H6 (pyrimidine) or H1′–H8 (purine) connectivity for the assignments. Labels show the intraresidual H1′–H6 or H1′–H8 signals of each residue. Green, cyan and purple lines represent the sequential walk of the segments shown in the same colors in (**a**). Asterisks indicate that the signals are below the threshold. (**e**) ^{1}H-^{1}H NOESY spectrum of [u-^{2}H, {H1′,H2′,H2,H8}-Ade] ΔJΔK in H_2O. (**f**) Regions of ^{1}H-^{1}H NOESY spectra of unlabeled ΔJΔK (top) and [u-^{2}H, ^{1}H-Ade/Gua] ΔJΔK (bottom). (**g-i**) Regions of ^{1}H-^{1}H NOESY spectra showing the NOE connectivities from the A_{SL} to the J and K domains. (**j**) A region of ^{1}H-^{1}H NOESY spectrum of [u-^{2}H, {H1′,H2′,H2,H8}-Ade] ΔJΔK in H_2O. The long range connectivities that shows the register of the A_{SL} to the J and K domains are labeled in red.

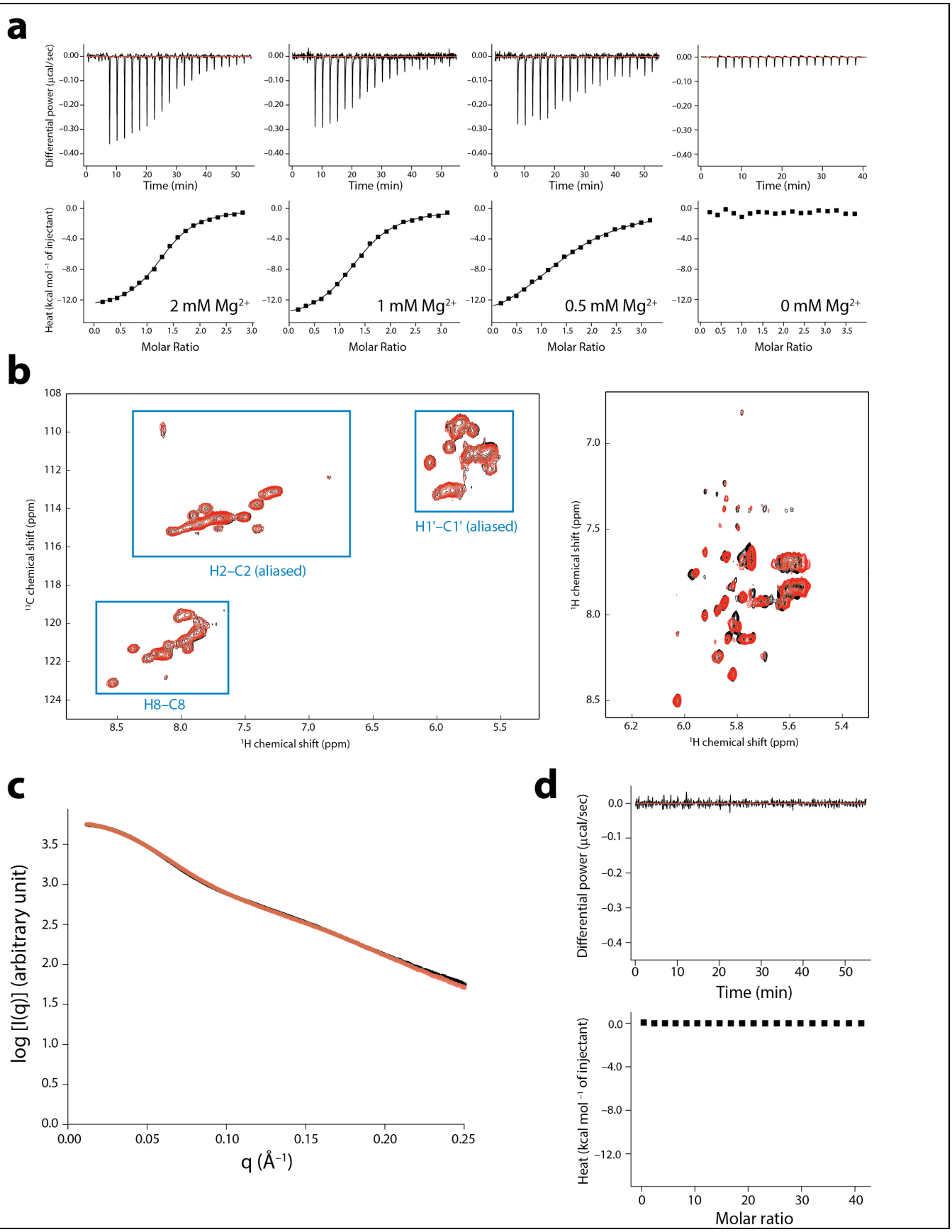
a
Differential power (µcal/sec)
Time (min)
Heat (kcal mol⁻¹ of injectant)
Molar Ratio
2 mM Mg2+
1 mM Mg2+
0.5 mM Mg2+
0 mM Mg2+
b
13C chemical shift (ppm)
1H chemical shift (ppm)
H2–C2 (aliased)
H1'–C1' (aliased)
H8–C8
c
log [I(q)] (arbitrary unit)
q (Å−1)
d
Differential power (µcal/sec)
Time (min)
Heat (kcal mol⁻¹ of injectant)
Molar ratio

Supplementary Figure 5

Mg^{2+} concentration dependence of the J-K–HEAT-1 interaction

(**a**) Results of ITC experiments in which the HEAT-1 domain was titrated to the J-K region at 2, 1, 0.5, and 0 mM of Mg^{2+}. The interaction between the J-K region and the HEAT-1 domain requires divalent ions as seen by the lack of heat of interaction in the absence Mg^{2+} ions. (**b**) NMR spectral overlay. Left: Overlay of the ^{1}H-^{13}C HMQC spectra of [^{13}C,^{15}N-Ade] J-K in the absence (black) and presence of 1 mM Mg^{2+} (red). Right: Overlay of the ^{1}H-^{1}H NOESY spectra of [u-^{2}H, {H1′,H2′,H2,H8}-Ade] J-K in the absence (black) and presence of 1 mM Mg^{2+} (red) (**c**) SAXS profiles of the J-K region in the absence (black) and presence of excess (2 mM) Mg^{2+} (red). (**d**) Results of the ITC experiment in which Mg^{2+} was titrated to the J-K region.

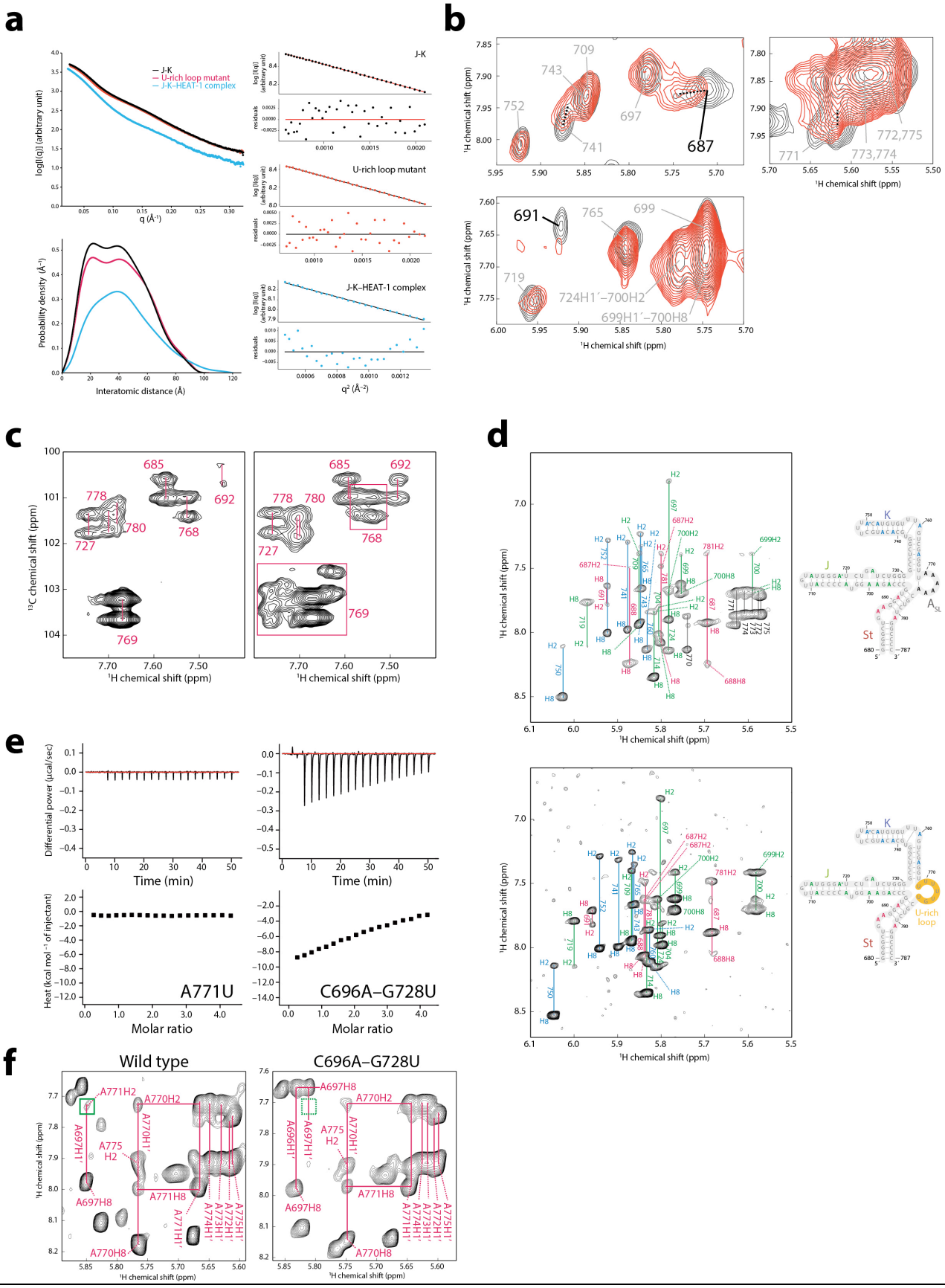
a
J-K
U-rich loop mutant
J-K–HEAT-1 complex
log[I(q)] (arbitrary unit)
q (Å⁻¹)
Probability density (Å⁻¹)
Interatomic distance (Å)
residuals
q² (Å⁻²)
b
¹H chemical shift (ppm)
709
743
752
741
697
687
772,775
771
773,774
691
765
699
719
724H1′–700H2
699H1′–700H8
c
¹³C chemical shift (ppm)
685
692
778
780
768
727
769
d
e
Differential power (µcal/sec)
Time (min)
Heat (kcal mol⁻¹ of injectant)
Molar ratio
A771U
C696A–G728U
f
Wild type
C696A–G728U
A771H2
A770H2
A697H1′
A775 H2
A770H1′
A771H8
A697H8
A770H8
A696H1′
A775 H2
A697H8H8

Supplementary Figure 6

SAXS, NMR, and ITC data

(**a**) Results of the SAXS analyses. Top left: The intensity plots of SAXS data of the J-K region (black), U-rich loop mutant (red), and J-K–HEAT-1 domain complex (cyan). I is scattering intensity, q is proportional to the scattering angle ($q = 4\sin\theta/\lambda$, where 2θ is the angle between the incident x-ray beam and the detector, and λ is x-ray wavelength in Å). Right: The Guinier plots of the J-K region, U-rich loop mutant, and J-K–HEAT-1 domain complex. The linear least square fitting provided the radius of gyration of 28.9 ± 0.1, 29.6 ± 0.1, and 34.9 ± 0.1 Å for the J-K region, U-rich loop mutant, and J-K/HEAT-1 domain complex, respectively. Bottom left: The pairwise distance distribution function (PDDF) plots of the J-K region (black), U-rich loop mutant (red), and J-K–HEAT-1 domain complex (cyan), respectively. (**b**) NMR titration experiment. ^{1}H-^{1}H NOESY spectra of [u-^{2}H, {H1′,H2′,H2,H8}-Ade] J-K region in the absence (black) and substoichiometric presence (red) of the HEAT-1 domain, shown as in Fig. 5b. Assignments of the intraresidual H1′–H8 NOE signals are labeled with the residue numbers, whereas strong intraresidual NOE correlation between H2 and H1′ are labeled with residue numbers and atom names. Residues whose NOE signal intensities were substantially reduced by the addition of the HEAT-1 domain are labeled in black, as in Fig. 5b. (**c**) Temperature dependent NMR spectral change of ΔJΔK. Left: The H6–C6 region of ^{1}H-^{13}C HMQC spectrum of ΔJΔK at 35ºC. The H6–C6 signal of U769 is down-field shifted in the ^{13}C dimension, indicating that it adopts the *syn* conformation. Right: The same region of the spectrum at 45ºC. The H6–C6 signals of U768 (at the bottom of the K domain) and U769 (one of the residue from the closing basepair of A_{SL} domain) are split, whereas the others are not. (**d**) ^{1}H-^{1}H NOESY spectra of the wild type and U-rich loop mutant of the J-K region. Top: ^{1}H-^{1}H NOESY spectrum of [u-^{2}H, {H1′,H2′,H2,H8}-Ade] J-K. Bottom: ^{1}H-^{1}H NOESY spectrum of [u-^{2}H, {H1′,H2′,H2,H8}-Ade] U-rich loop mutant. H1′ resonances are shown with vertical lines with the intraresidual NOE signals labeled as H2 and H8. Interresidual NOE signals from each H1′ resonance are labeled with residue numbers. Labels and lines are colored red (St), green (J), cyan (K), and gray (A_{SL}), depending on the domains that belong to. In each panel, the secondary structure is shown on the right with the mutated stretch highlighted in orange. (**e**) Results of ITC experiments where the HEAT-1 domain was titrated to the A771U and C696A/G728U mutant of the J-K region. (**f**) ^{1}H-^{1}H NOESY spectra of the wild type and C696A/G728U of [u-^{2}H, {H1′,H2′,H2,H8}-Ade] ΔJΔK. Although signals from the A_{SL} domain residues (A770-A775) were not perturbed, the long range NOE between A771 H2 (A_{SL}) and A697 H1′ (J) disappeared (green boxes), indicating that the long range interaction between the A_{SL} and J domains is abrogated by the mutation.

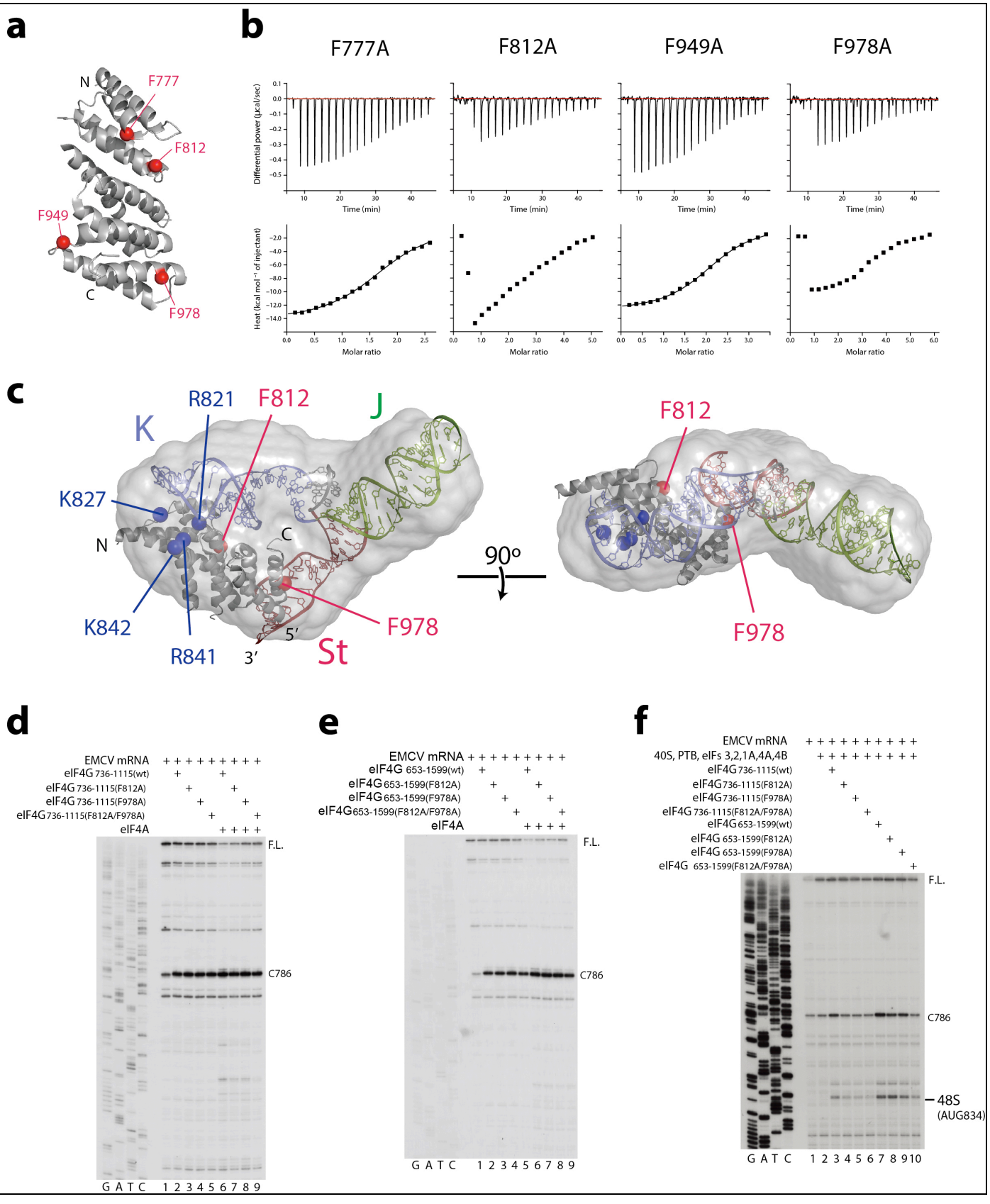
a
N
F777
F812
F949
C
F978
b
F777A
F812A
F949A
F978A
Differential power (µcal/sec)
Time (min)
Heat (kcal mol⁻¹ of injectant)
Molar ratio
c
R821
F812
J
K
K827
N
C
K842
R841
3′
5′
St
F978
90°
F812
F978
d
EMCV mRNA
eIF4G 736-1115(wt)
eIF4G 736-1115(F812A)
eIF4G 736-1115(F978A)
eIF4G736-1115(F812A/F978A)
eIF4A
F.L.
C786
G A T C 1 2 3 4 5 6 7 8 9
e
EMCV mRNA
eIF4G 653-1599(wt)
eIF4G653-1599(F812A)
eIF4G653-1599(F978A)
eIF4G653-1599(F812A/F978A)
eIF4A
F.L.
C786
G A T C 1 2 3 4 5 6 7 8 9
f
EMCV mRNA
40S, PTB, eIFs 3,2,1A,4A,4B
eIF4G736-1115(wt)
eIF4G736-1115(F812A)
eIF4G736-1115(F978A)
eIF4G 736-1115(F812A/F978A)
eIF4G653-1599(wt)
eIF4G 653-1599(F812A)
eIF4G 653-1599(F978A)
eIF4G 653-1599(F812A/F978A)
F.L.
C786
48S
(AUG834)
G A T C 1 2 3 4 5 6 7 8 9 10

Supplementary Figure 7

Structure model of the J-K–HEAT-1 domain complex and mutagenic analyses

(**a**) Positions of exposed aromatic residues on the HEAT-1 domain. Conserved and exposed aromatic residues of the eIF4G1 HEAT-1 domain are mapped onto the crystal structure of the homologous eIF4G2 (PDB ID: 1HU3). (**b**) Results of the ITC experiments of the interaction of F777A, F812A, F949A, and F978A HEAT-1 domain mutants with the J-K region. (**c**) Structure model of the J-K–HEAT-1 domain complex derived from the SAXS, NMR, and previous mutagenesis assay. Structures of the J-K region and the eIF4G2 HEAT-1 domain (PDB ID: 1HU3) are placed into the SAXS *ab initio* envelope structure (gray). The basic residues previously identified to be involved in the interaction (R821, K827, R841, and K842) are shown with blue spheres (**d,e**) The results of assaying formation of binary eIF4G–IRES and ternary eIF4G–eIF4A–IRES complexes by eIF4G(736-1115) (**d**) and eIF4G(653-1599) (**e**). The bands labeled as C786 and F.L. represent the fall-off of the reverse transcriptase (RT) at C786 by the binding of eIF4G to the J-K region, and the full-length cDNA where the RT is not stopped by the eIF4G–IRES complex, respectively. (**f**) The results 48S complex formation assays by eIF4G(736-1115) (lanes 3-6) and eIF4G(653-1599) (lanes 7-10). The 48S formation is evidenced by the bands labeled as 48S(AUG834), which reflects the fall-off of the RT by the 48S complex formed at the first codon(AUG834).